Effect of Heating Rate on the Melting Behavior of the Alloy 53Nb-47Ti (Mass %) in Rapid Pulse-Heating Experiments[1]

A. Cezairliyan,[2,3] W. J. Boettinger,[2] D. Basak,[2] D. Josell,[2] and J. L. McClure[2]

---

[1] Paper presented at the Thirteenth Symposium on Thermophysical Properties, June 22-27, 1997, Boulder, Colorado, U.S.A.

[2] Metallurgy Division, National Institute of Standards and Technology, Gaithersburg, Maryland 20899, U.S.A.

[3] To whom correspondence should be addressed.

ABSTRACT

Experiments were conducted to study the effect of heating rate on the melting behavior of the binary alloy 53Nb-47Ti (mass %). The method is based on rapid resistive self-heating of the specimen from room temperature to its melting region by the passage of an electrical current pulse through it and on measuring surface radiance temperature and normal spectral emissivity of the specimen as a function of time. Radiance temperature was measured with a high-speed pyrometer; normal spectral emissivity was measured with a high-speed laser polarimeter. The pulse heating time (time to heat the specimen from room temperature to the melting onset temperature) ranged from 120 to 6300 ms, which corresponds approximately to a heating rate close to the melting region of 12 to 0.1 $K \cdot ms^{-1}$. The results indicate that the onset of melting of the alloy 53Nb-47Ti, in contrast to a pure metal, depends significantly on heating rate. Various aspects of non-equilibrium melting and implications for future research are discussed.

KEY WORDS: alloys; high-speed measurements; high temperatures; melting; niobium; niobium-titanium alloy; pulse heating; titanium.

1. INTRODUCTION

In contrast to a pure metal, which melts at a constant temperature (for fixed pressure), an alloy melts over a temperature range bounded by the solidus and liquidus temperatures. Both solidus and liquidus temperatures are well-defined thermodynamic quantities and can be measured under equilibrium conditions. However, when an alloy melts sufficiently rapidly it is possible that, like a pure metal, it will melt at a single thermodynamically defined temperature which falls between the solidus and liquidus.

The objective of the present paper is to report and discuss the results of an experimental study on the melting behavior of the binary alloy 53Nb-47Ti (mass %) as a function of heating rate. The pulse heating time (time to heat the specimen from room temperature to the melting onset temperature) ranged from 120 to 6300 ms, which corresponds approximately to a heating rate close to the melting region of 12 to 0.1 $K \cdot ms^{-1}$.

2. MELTING OF ALLOYS

To obtain equilibrium in a melting alloy, diffusion of solute must be sufficiently fast compared with the melting to ensure uniform concentrations in each phase. Under equilibrium conditions, the enthalpy-versus-temperature curve exhibits an abrupt increase in slope at the solidus, a smooth curve to the liquidus temperature, and an abrupt decrease in slope at the liquidus. This complete equilibrium is usually quite difficult to achieve for solid metallic phases, where solute diffusion in substitutional solid solutions, D_S, is typically four orders of magnitude slower than diffusion in liquid phases, D_L.

The T_0 temperature is defined (see Ref. [1]) as the temperature where liquid and solid phases of the same given composition have equal free energies. The T_0 temperature always lies between the liquidus and solidus temperatures. It is relevant to melting and freezing processes that proceed at such high rates that there is no time for redistribution of solute between the liquid and solid phases by diffusion. Under this restriction, it is the

lowest temperature at which melting can occur during heating and the highest temperature at which freezing can occur during cooling. It is thus similar to the melting point of a pure metal. Under this constrained equilibrium, the enthalpy-versus-temperature curve is identical in shape to that of a pure metal with the T_0 temperature acting as the melting/freezing point. Thus in this limit, one would anticipate temperature-versus-time curves on heating of an alloy with a plateau at the T_0 temperature.

The values of the cooling rates (more properly the liquid/solid interface speeds), required to achieve T_0 solidification is the subject of rapid solidification research [2, 3]. Under rapid solidification processes, a continuous kinetic change is observed from "equilibrium" freezing to "near T_0" freezing as the solidification speed is increased to a speed of the order of D_L/d, where d is the interface thickness. For $D_L=10^{-5}$ $cm^2 \cdot s^{-1}$ and d $=10^{-7}$ cm, one obtains a characteristic speed of the order of 10^2 $cm \cdot s^{-1}$. The authors are unaware of any publication on T_0 melting. Nonetheless, one might expect that on melting, such an effect would occur when the melt front velocity is greater than the characteristic melting speed D_S/d. With $D_S=10^{-9}$ $cm^2 \cdot s^{-1}$, the characteristic speed would be 10^{-2} $cm \cdot s^{-1}$.

3. MEASUREMENT METHOD

The method for studying the melting behavior of an alloy is based on rapid resistive self-heating of the specimen from room temperature to the melting region in short times by the passage of an electrical current pulse through it; and on measuring, with millisecond resolution, normal spectral emissivity of the specimen and surface radiance temperature of the specimen. The normal spectral emissivity (at 633 nm) of the specimen was measured with a high-speed laser polarimeter [4]. The surface radiance temperature of the specimen at 633 nm was determined (by linear interpolation) from measurements of the surface radiance temperatures at two bracketing wavelengths, 624 and 651 nm, with two high-speed solid-state pyrometers [5, 6]. True temperature of the specimen was then determined from the data on surface radiance temperature and normal spectral emissivity, both corresponding to

the same wavelength, using Planck's law. The experimental quantities were recorded simultaneously with a high-speed digital data acquisition system having 16-bit resolution. Details regarding construction and operation of the original measurement system, the methods of measuring experimental quantities, and other pertinent information are given in earlier publications [7, 8]. A recent significant modification to the system involving a computer-controlled solid-state switch for the control of the current through the specimen is described elsewhere [9].

4. MEASUREMENTS

4.1. Specimens

The 53 Nb-47 Ti (mass %) specimens were nominally 1.6 mm in diameter and 73 mm in length. As reported by the manufacturer, the alloy material contained the following major impurities (ppm by mass): 1200 Ta, 600 O, and 100 each Hf, Si, and Zr, with total remaining 500 ppm of other elements. The specimens were polished with #600 abrasive paper to provide a reproducible and smooth surface for both pyrometric and polarimetric measurements.

Before the experiments, the as-received specimens were heat treated by pulse heating them to a surface radiance temperature of 1920 K (approximately 2090 K in true temperature) and holding them at that temperature for about 1.5 s. The heavily deformed structure of the as-received drawn wire was converted to an equiaxed grain structure by the heat treatment.

The relative amounts of Nb and Ti and distribution within the specimens were determined at NIST with a scanning electron microscope by Energy Dispersive Spectroscopy using elemental standards. Three as-received specimens from different parts of the alloy wire were cross sectioned transverse to the wire axis, polished by standard metallographic techniques and analyzed for composition at one hundred points along a diameter of each cross section. The average compositions were consistent with the

±1 mass % variation about 47 mass % Ti specified by the manufacturer of the wire. However, all three locations exhibited Ti enrichment toward the center and surface of the wire, with Nb enrichment a maximum at approximately one half the wire radius; such radial composition variation can be expected in cast and drawn wires. The maximum composition variation associated with this macrosegregation was approximately 1 mass %. The heat treatment of the wires to remove the heavily deformed drawing structure did not alter these profiles significantly.

4.2. Experiments

A total of 13 experiments were performed on 13 alloy specimens. After heat treatment, each specimen was pulse heated to its melting region at a different heating rate. The heat treatment and pulse heating experiments were conducted with the specimen in an argon (99.999% pure) environment at a slightly above atmospheric pressure. The pulse heating time for different experiments ranged from 120 to 6300 ms, which corresponds approximately to a heating rate close to the melting region of 12 to 0.1 $K \cdot ms^{-1}$. In order to compare the melting behavior of the alloy with that of its constituent elements, experiments were also performed on a Nb and a Ti specimen (each 99.9+ % pure).

A set of six (two pyrometry and four polarimetry) experimental quantities were recorded simultaneously with the digital data acquisition system at rates in the range 0.5 to 4 kHz, depending on the heating rate. The pyrometry data yielded surface radiance temperatures at 624 and 651 nm and the polarimetry data yielded normal spectral emissivity at 633 nm, wavelength of the helium-neon laser in the polarimeter. From the above data, in conjunction with Planck's law, it was possible to determine the true temperature of the specimen at any given point. All temperatures reported in this paper are based on the International Temperature Scale of 1990 [10].

5. EXPERIMENTAL RESULTS

The results of a typical pulse heating experiment are presented in Fig. 1, where both surface radiance temperature and normal spectral emissivity at 633 nm of the specimen are plotted as a function of pulse heating time. The heating duration can be divided into the following three regions: Region I, where the entire specimen is in the solid phase, Region II, where bulk of the specimen is in the solid phase yet a thin surface layer undergoes a change (possibly melting), and Region III, where bulk of the specimen undergoes melting. Transition from Region I to II is marked by a "kink" in the surface radiance temperature trace and a corresponding sharp decrease in the normal spectral emissivity trace. Transition from Region II to III is marked by a significant reduction in the slope of the radiance temperature trace indicative of the onset of bulk melting, with no further change in the emissivity trace. The mid-point (also usually the inflection point) value of the kink was taken as the kink temperature. When the surface radiance temperature is converted to true temperature using the measured value of normal spectral emissivity, the kink almost entirely disappears on the temperature-versus-time plot. The fact that there is insignificant latent heat suggests that the kink is largely due to a surface effect. The melting onset temperature was determined from the intersection of the linear extrapolation of the surface radiance temperature traces corresponding to the rapid heating before the onset and the slow heating after the onset. Despite its slope, the region of slow heating, will be referred to as the “plateau” for the remainder of this paper. Clearly, this plateau corresponds to bulk melting.

The results of the kink and melting onset temperatures as a function of pulse heating time for the 13 experiments are presented in Fig. 2. The same results, plotted as a function of specimen heating rate, are shown in Fig. 3. It can be seen that the kink temperature is essentially independent of the pulse heating time, i.e. the heating rate, while the melting onset temperature shows a definite dependence on the pulse heating time. The horizontal lines in Figs. 2 and 3 represent the average kink temperature (standard deviation 1.2 K) for the 13 experiments. The melting onset temperatures for the 13 experiments, as seen in Fig.

2, were fitted (standard deviation 0.9 K) by a linear function using the least squares method. Conversion of radiance temperature to true temperature yields a value of 2141 K for the average kink temperature and 2201 K for the melting onset temperature for the specimen with the highest heating rate. No kink was observed before melting for either pure Ti or Nb. The estimated uncertainties (two-standard deviation level) in measured surface radiance temperature and true temperature are 5 and 7 K, respectively [4, 7].

Auxiliary experiments were performed where specimens were heated to following temperatures: (a) just below the kink, (b) above the kink but below the plateau, (c) early on the plateau and (d) later on the plateau. Specimens were examined by optical and scanning electron microscopy (SEM). Microscopy of specimen surfaces (Fig. 4) indicated that the surface of (a) still exhibited surface roughness from its preparation with #600 abrasive paper; this roughness disappeared from the surface of (b) (consistent with the measured decrease of the emissivity at the kink) and some shallow grain boundary grooves the were now evident. On the surface of (c) and (d) there were, in addition to deeper grain boundary grooves, structures that had clearly been melted and then resolidified at some triple junctions and grain boundaries (consistent with the melting plateau). Optical microscopy of cross sectioned specimens indicated equiaxed grains in all specimens but showed voids and other microstructure in the specimens heated to the plateau (c, d) . These structures are consistent with melting and resolidification in the interior of the specimen.

Compositional analysis in the scanning electron microscope of the cross sectioned specimens indicated segregation of Ti (3 to 6 mass % Ti enrichment) to grain boundary regions only in specimens that had been heated onto the plateau (c, d).

6. DISCUSSION

The solidus temperature of the 53 Nb-47 Ti alloy (2100 K) is based on limited data, and the liquidus has been computed as 2160 K [11]. From the solidus curve, 1 mass %

variation in local composition could contribute an uncertainty of approximately 6 K in the solidus temperature. This is much smaller than the observed separation between kink and melting onset temperatures for all the heating rates examined.

Two issues to be addressed are the meaning of the melting onset temperature and the reason for the change of emissivity creating the "kink" on the radiance temperature plots prior to attainment of the melting plateau. It is proposed that the plateau indicates melting of the bulk sample at temperatures approaching T_0 with increasing heating rate. It is also proposed that the kink is caused by melting of the sample surface when the temperature reaches that of the solidus for the bulk alloy. It should be noted that if these features do in fact correspond to these phenomena then these heating experiments provide two fundamental temperatures for the thermodynamic determination of phase diagrams.

As seen in Fig. 3, at heating rates $\dot{T}$ greater than 3 $K \cdot ms^{-1}$, the melting onset temperature becomes essentially independent of heating rate. This is strong evidence that this value of the melting onset temperature has a thermodynamic character. Assuming that melting always is initiated at grain boundaries (and the specimen surface), a simple estimate for the initial melting speed can be obtained from the heating rate. For spherical grains of radius, R, the initial rate of change of the volume fraction of liquid is 3V/R, where V is the melting speed. But at constant temperature (i.e., for times on the plateau) , the rate of change of the volume fraction of liquid is also given by $C_P \dot{T}/\Delta h_f$ where C_P and Δh_f are the heat capacity of the solid and heat of fusion, respectively. One then obtains that $V=RC_P \dot{T}/(3\Delta h_f)$. The velocity would increase as the melt front moves toward the center of the grains. For an average grain radius typical of the specimens of 30 μm (see Fig. 4) and a value of $\Delta h_f/C_P$ of 500 K, the speed V corresponding to 3 $K \cdot ms^{-1}$ is of the order 10^{-2} $cm \cdot s^{-1}$. This agrees with the estimate D_S/a obtained in Sect. 2. Thus, it seems reasonable that the melting onset temperature obtained at the highest heating rates is near the T_0 temperature for this alloy composition. It is also believed that the segregation observed at the grain

boundaries in the specimens heated to the plateau occurred during resolidification, where the speeds required for T_0 freezing would not be obtained by the relatively slow cooling rate of the specimens, rather than during melting.

The origin of the sharp drop in normal spectral emissivity at a temperature below the plateau is less clear. The observation (Fig. 1) that normal spectral emissivity remains essentially the same in Regions II and III suggests that the specimen has developed a thin molten surface layer in Region II. A molten surface could smooth itself in millisecond time scales. However, one must ask why the surface melts at a lower temperature than the bulk. The simplest idea would involve a small amount of melting at the solidus, an idea consistent with the heating rate independence of the kink temperature. For solidus melting, a liquid must be formed which is richer in Ti than the solid (according to the tie line of the phase diagram). To conserve solute locally, this process requires a decrease in Ti content of the remaining solid near the melting interface. Such a process requires solid diffusion. In the several milliseconds associated with the kink, the depth of the solid where the Ti content could be lowered cannot exceed $(D_s t)^{1/2}$ or ~20 nm. The thickness of the melted region would be similar. Further melting would be kinetically limited by the slowness of the solid diffusion until the temperature attains T_0 where the requirement to form liquid rich in Ti is not required. The proposed ~20 nm thick Ti-rich regions on the sample surface and at the grain boundaries would be difficult to detect by the SEM analysis performed here. Such a mechanism would explain the smoothing of the sample surface, the slight delineation of the grain boundaries observed in Fig. 4b and the temperature independence of the kink temperature. This mechanism, which is based on the difficulty of solute diffusion in the solid, is consistent with the fact that this effect was not observed with specimens of pure Ti or Nb.

Despite our analysis, there is a possibility that the limiting value of the melting onset temperature at the highest heating rate is the liquidus temperature of the alloy and not the

T_0 temperature. Future experiments are planned to extend conditions to both slower and faster heating rates and to use an alloy whose liquidus and solidus temperatures are more clearly established. The slower experiments should approach equilibrium conditions and thus help clarify the relationship between the kink temperature and the solidus temperature. The faster experiments should more conclusively establish the achievement of T_0 melting.

REFERENCES

1. J.C. Baker and J. W. Cahn, in *Solidification* (ASM, Metals Park, OH, 1971), p. 23.

2. M.J. Aziz and W. J. Boettinger, Acta Metall. Mater.**42**: 527 (1994).

3. M.J. Aziz, Met. Trans.27A: 671 (1996).

4. A. Cezairliyan, S. Krishnan, and J. L. McClure, Int. J. Thermophys. 17: 1455 (1996).

5. E. Kaschnitz and A. Cezairliyan, Int. J. Thermophys. 17: 1069 (1996).

6. A. Cezairliyan, G. M. Foley, M. S. Morse, and A. P. Miiller, in Temperature - Its Measurement and Control in Science and Industry, Vol. 6, J. F. Schooley, ed. (AIP, New York, 1992), pp. 757-762.

7. A. Cezairliyan, M. S. Morse, H. A. Berman, and C. W. Beckett, J. Res. Natl. Bur. Stand. (U.S.) 74A: 65 (1970).

8. A. Cezairliyan, J. Res. Natl. Bur. Stand. (U.S.) 75C: 7 (1971).

9. T. Matsumoto and A. Cezairliyan, Int. J. Thermophys. 18: xxxx (1997).

10. H. Preston-Thomas, Metrologia 27: 3 (1990); 27: 107 (1990).

11. J. L. Murray, in *Phase Diagrams of Binary Titanium Alloys*, J. L. Murray, ed. (ASM International, Metals Park, OH, 1987), p.188.

FIGURE CAPTIONS

Fig. 1. Surface radiance temperature and normal spectral emissivity at 633 nm of a 53 Nb-47 Ti (mass %) specimen as a function of time during rapid heating to its melting region.

Fig. 2. Surface radiance temperatures corresponding to the kink and melting onset of thirteen 53 Nb-47 Ti (mass %) specimens for different pulse heating times (the time to heat the specimen from room temperature to the melting onset temperature).

Fig. 3. Surface radiance temperatures corresponding to the kink and melting onset of thirteen 53 Nb-47 Ti (mass %) specimens heated at different rates. Heating rate is evaluated at a temperature a few degrees below the kink.

Fig. 4. SEM photomicrographs showing the surface morphologies of 53 Nb - 47 Ti (mass %) specimens heated to the following temperatures: (a) just below the kink, (b) above the kink but below the plateau, (c) early on the plateau and (d) later on the plateau.

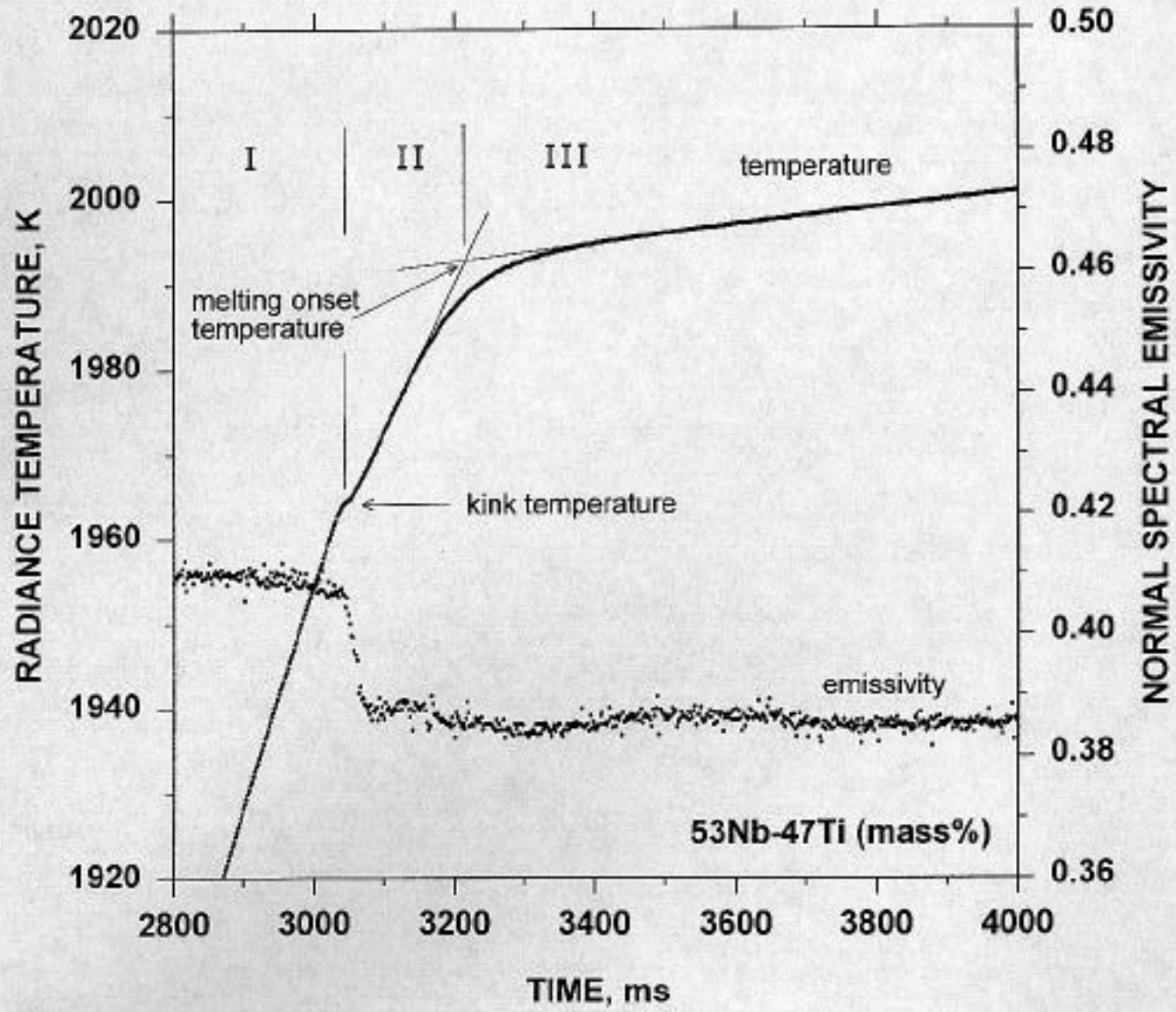
2020
2000
1980
1960
1940
1920
RADIANCE TEMPERATURE, K
0.50
0.48
0.46
0.44
0.42
0.40
0.38
0.36
NORMAL SPECTRAL EMISSIVITY
2800
3000
3200
3400
3600
3800
4000
TIME, ms
I
II
III
temperature
melting onset
temperature
kink temperature
emissivity
53Nb-47Ti (mass%)

Figure 1

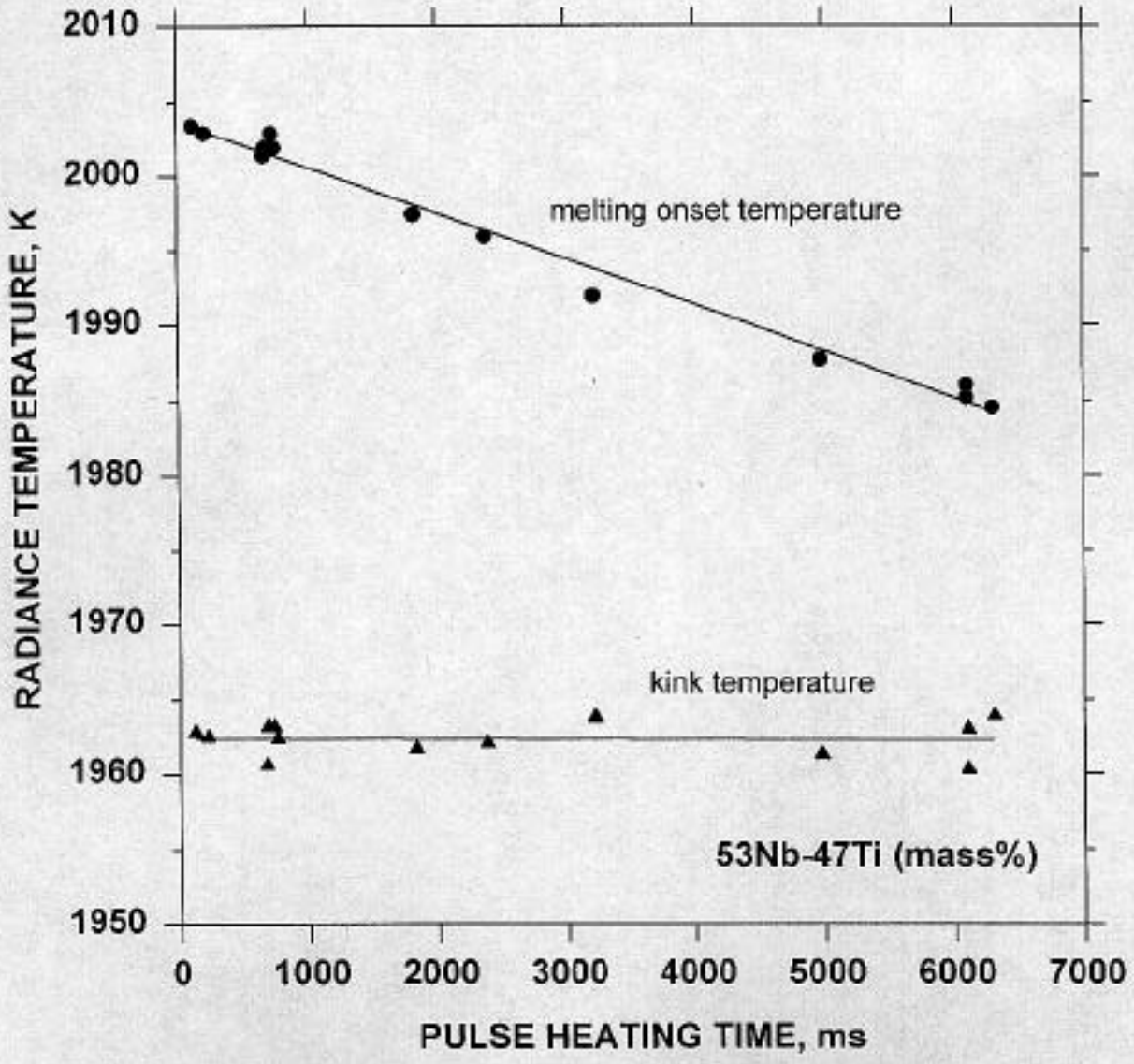
2010
2000
1990
1980
1970
1960
1950
RADIANCE TEMPERATURE, K
melting onset temperature
kink temperature
53Nb-47Ti (mass%)
0
1000
2000
3000
4000
5000
6000
7000
PULSE HEATING TIME, ms

Figure 2

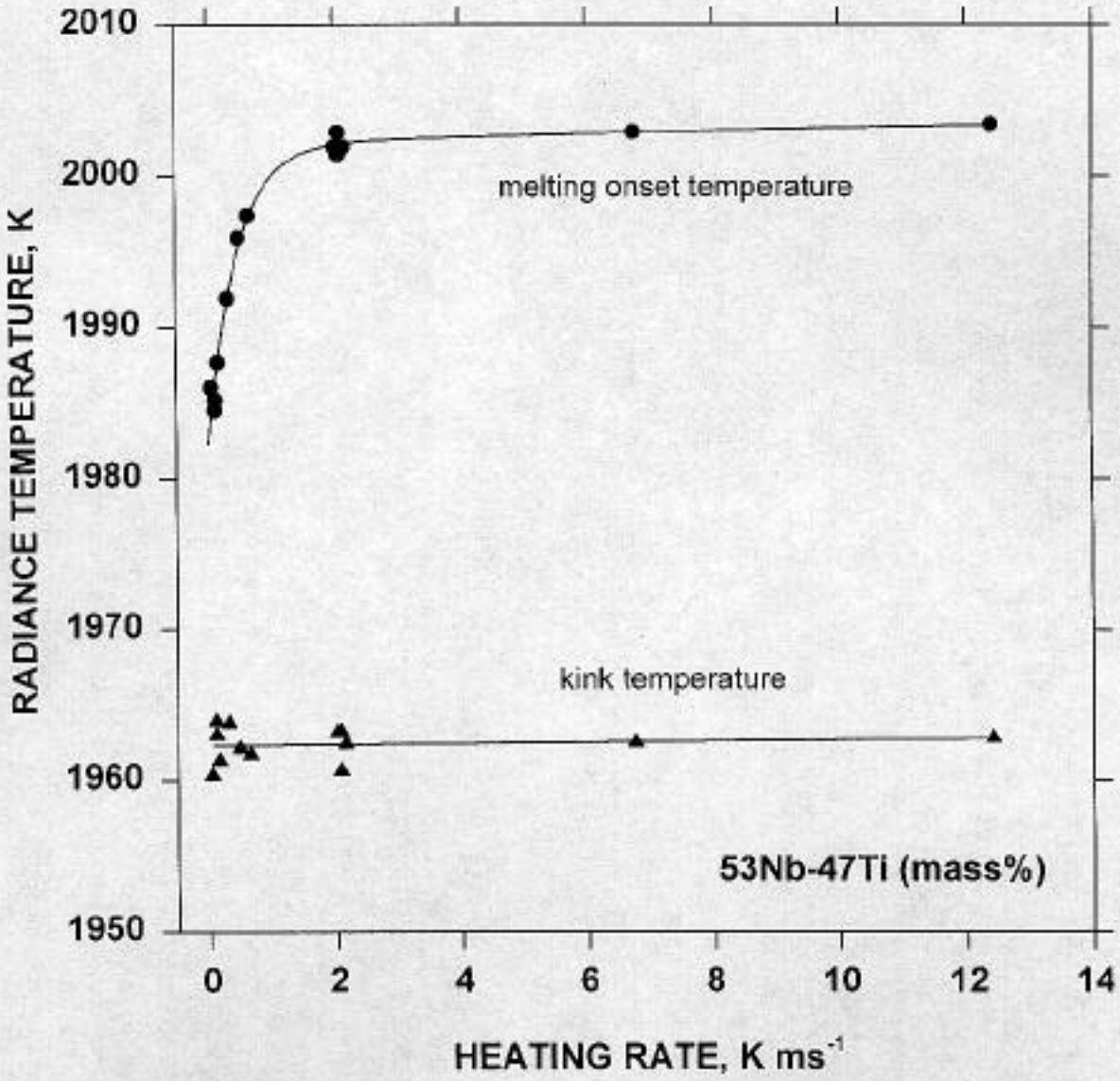
2010
2000
1990
1980
1970
1960
1950
RADIANCE TEMPERATURE, K
melting onset temperature
kink temperature
53Nb-47Ti (mass%)
0
2
4
6
8
10
12
14
HEATING RATE, K ms^{-1}

Figure 3

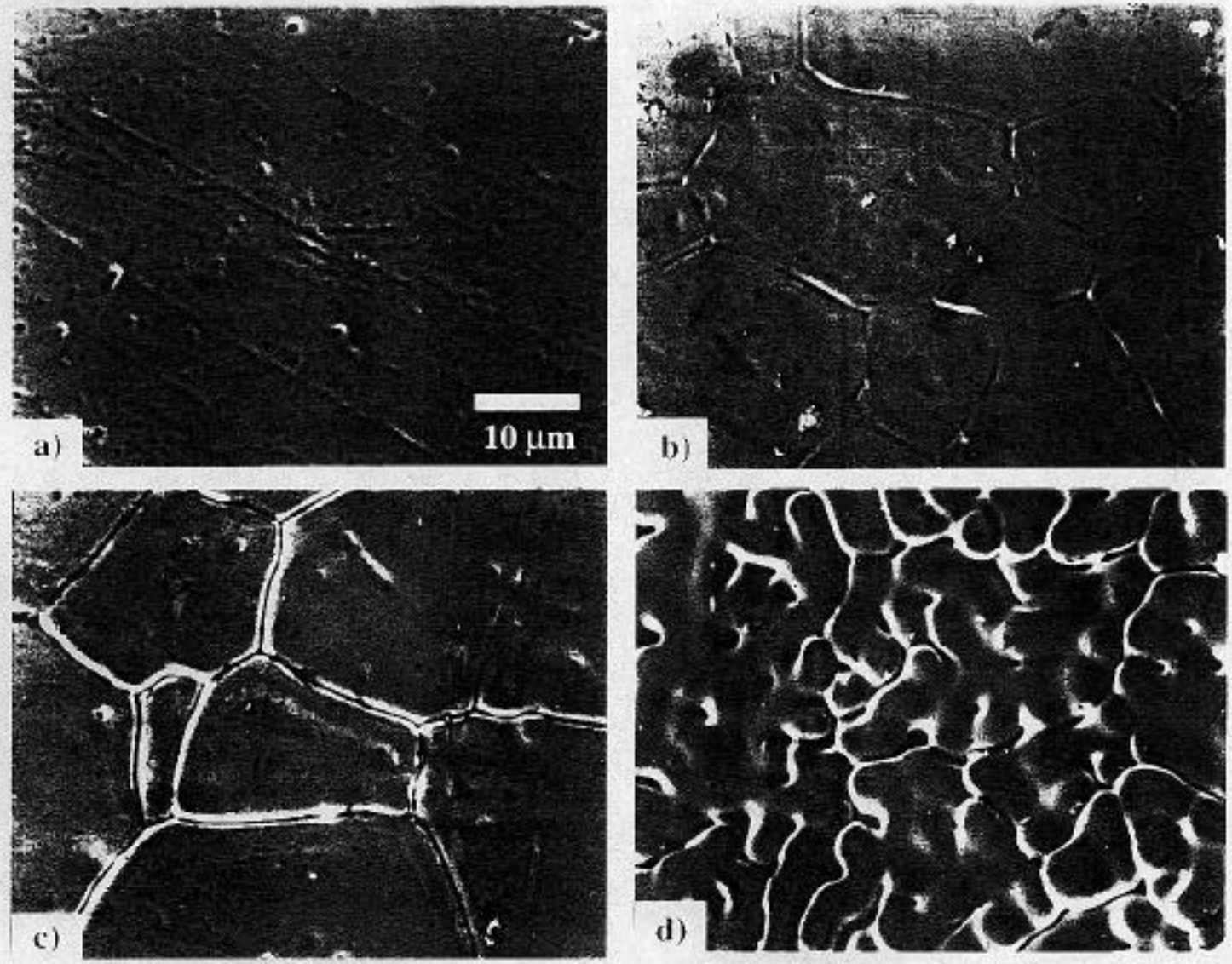

Figure 4